

BEAM CONFINEMENT DYNAMICS IN A BARRIER BUCKET

*Masatake Hirose^{A,B)}, Ken Takayama^{A,B,C,D)}, Takashi Yoshimoto^{B,C)}, Liu Xiggung^{B,C)}

^{A)}Tokyo City University, Tamatsutsumi, Setagaya, Tokyo, Japan

^{B)}High Energy Accelerator Research Organization (KEK), Tsukuba, Ibaraki, Japan

^{C)}Tokyo Institute of Technology, Nagatsuda, Yokohama, Kanagawa, Japan

^{D)}The Graduate University for Advanced Studies (SOKENDAI), Hayama, Kanagawa, Japan

Abstract

In an induction synchrotron such as the KEK digital accelerator, the barrier voltage pulse with almost rectangular shape is generated in an induction cell of a 1-to-1 pulse transformer driven by the switching power supply. Its peak amplitude and pulse length are flexibly changed but the rising/falling time is uniquely determined by a combination of the circuit parameters including characteristics of the employed solid-state switching element. Behavior of particles captured in the barrier bucket is quite various, depending on the barrier voltage shape. This paper systematically discuss about the phenomenology of beam dynamics for the barrier bucket and compare numerical simulations with the experimental results obtained in the KEK digital accelerator.

INTRODUCTION

Beam handling using the barrier bucket has been initiated by Jim Griffin of Fermilab in 1983, where the barrier voltage was obtained by superimposing multiple harmonic RFs[1]. The stability region in the phase space that the barrier voltage made came to be called an isolated bucket. However, it is hard to realize almost square pulse in a high-Q cavity, because, a large number of harmonics are needed. This technique has evolved since then [2]. The barrier voltage was realized in the low-Q cavity where necessary number of harmonic waves for square pulse formation is reduced. By feeding the harmonic waves amplified by a semiconductor amplifier to the cavity, the beam handling using the barrier bucket was demonstrated [3].

On the other hand, in an induction synchrotron such as the KEK digital accelerator, the barrier voltage pulse with an almost rectangular shape is generated in an induction cell of a 1-to-1 pulse transformer driven by a switching power supply (SPS). Such an induction acceleration technique is equivalent to the RF acceleration. The induction acceleration has been successfully demonstrated in the slow-cycling and fast-cycling synchrotrons in KEK [4, 5]. The KEK digital accelerator is a fast-cycling induction synchrotron, which is shown in Fig. 1. The experiment of beam handling by the barrier bucket has been extensively conducted in the KEK digital accelerator.

The barrier voltage shown in Fig. 2 is generated by the induction acceleration system shown in Fig. 3. Pulse height V_{bb} of the barrier voltage is uniquely determined by setting the voltage of the DC power supply. Pulse length t_f

and barrier pulse duration T are determined by setting of timings (t_1, t_2, t_3, t_4), which manages the On/Off operation of the switching elements of the SPS. It is controlled by a program installed in Fields Programmed Gate Array (FPGA). Rising and falling times of the voltage pulse, t_{rise} and t_{off} , are determined by the intrinsic nature of the switching power supply including the circuit parameters and characteristics of the solid-state switching device. It is about 30 nsec in this case.

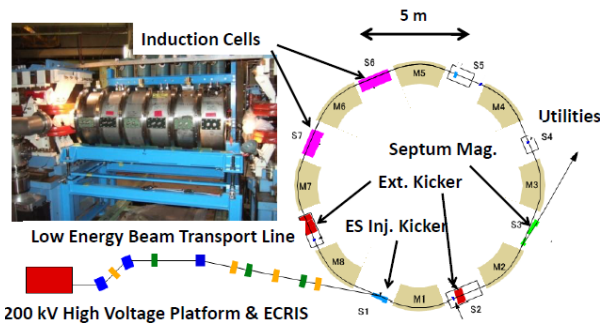


Figure 1: Schematic view of the KEK Digital Accelerator.

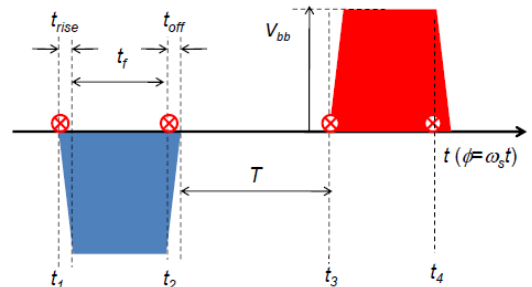


Figure 2: Barrier voltage pulses.

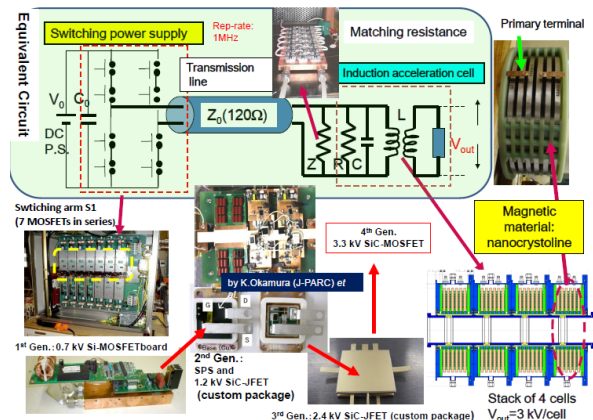


Figure 3: Equivalent circuit for the induction acceleration system.

CALCULATION OF PHASE SPACE ORBIT AND EMITTANCE

Longitudinal motion of the particles trapped in the barrier bucket is described by its energy E and phase ϕ whose evolutions for each turn are given by a recurrence formula, as shown in Equation (1). Since the applied voltage to the induction acceleration cell is time-dependent, the voltage seen by a particle is given by $V(\phi_n)$.

$$\begin{cases} E_{n+1} = E_n + QeV(\phi_n) \\ \phi_{n+1} = \left\{ \phi_n + 2\pi\eta \cdot \left(\frac{\Delta p}{p} \right) \right\}_{\text{mod } 2\pi} \end{cases} \quad (1)$$

$$\frac{\Delta p}{p} = \frac{\Delta E_n}{\beta_s^2 E_s} = \frac{E_n - E_s}{\beta_s^2 E_s} \quad (2)$$

$$\eta = \frac{1}{\gamma_T^2} - \frac{1}{\gamma_s^2} (< 0) \quad (3)$$

Where η is the momentum slippage factor and γ_T is the transition γ . Here, the parameters with suffix s are those of synchronous particle.

The longitudinal emittance is evaluated in terms of the following formula. The emittance defines it as the surface to include 95% of the particles.

$$\begin{aligned} \overline{s^2} &= \frac{1}{N} \sum_{i=1}^N s_i^2, \\ \overline{(E + \Delta E)^2} &= \frac{1}{N} \sum_{i=1}^N (E + \Delta E)_i^2, \\ \overline{s \cdot (E + \Delta E)} &= \frac{1}{N} \sum_{i=1}^N s_i \cdot (E + \Delta E)_i \end{aligned} \quad (4)$$

where s is distance from ideal particles and N is the number of particles.

$$\varepsilon = 4\sqrt{\overline{s^2} \cdot \overline{(E + \Delta E)^2} - (\overline{s \cdot (E + \Delta E)})^2} \quad (6)$$

COMPARISON BETWEEN EXPERIMENTS AND SIMULATIONS

The beam handling experiment has been conducted for the various amplitude and phase of the barrier voltage. The initial distribution in the phase space (ϕ, E) is shown in Fig. 4, where the uniform distribution is assumed in both directions with the maximum momentum error $(\Delta p/p)_{\text{max}}$ of 0.25 %.

Typical five cases of the barrier voltage have been experimentally studied, which are shown in the first row of Fig. 5. Each case is distinguished by the height V_{bb} and pulse length t_f of the barrier voltage pulse. It is noted that the actual voltage profile includes the main pulse with the rectangular shape, their reflections, and some overshoot

components. It is known later that these undesired voltage profiles induce asymmetric particle distributions.

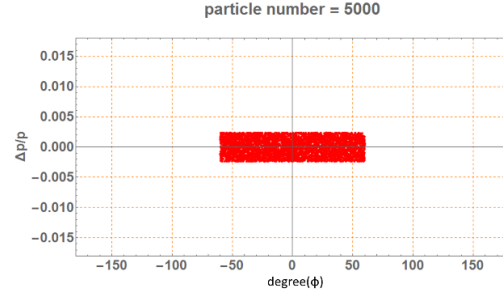


Figure 4: Initial distribution in the phase space ($\phi, \Delta p/p$).

Table 1: Each Parameters of Barrier Voltage

Case	V_{bb} (V)	t_f (ns)
A	1.200	200
B	1.000	1,200
C	1.200	1,000
D	5	4,000
E	50	4,000

The 2nd row of Fig. 5 represents the phase space structure of the individual case, which has been obtained by numerical tracking of test particles assumed in the phase space. The barrier bucket structures are clear. However, some of them are not symmetric due to a combination of asymmetric barrier voltage pulses. In addition, some of the buckets have their sub-structures. This means that a fraction of particles is trapped in such a substructure island.

The 3rd row denotes temporal evolutions of the macro particles of 5000, where the initial distribution is same among five cases and shown in Fig.4. The line density is projected on the 2D time space, time within a single revolution (horizontal) and time from injection (vertical).

The 4th row shows temporal evolutions of the beam bunch trapped in the barrier bucket, where the bunch signal obtained by the bunch monitor is projected on the 2D time space mentioned above. We can say that the simulation results are in a good agreement with the experimental results when the 3rd and 4th rows are compared.

The 5th row represents the change in time of the emittance defined by Eq. 6 for each case. Macroscopic oscillation is visible in Case B, C, and D. It is reasonable to understand that these phenomena are caused by mismatching of the injected bunch shape in the phase space to the waiting barrier bucket and a finite number of macro particles. Gradual increasing of the emittance is notable for Case A, B, and C, where the large barrier voltage is assumed. It has been known that the large barrier voltage reflects a particle entering the barrier region with a finite time step with an additional momentum. This is not found in Case D and E, where a lower barrier voltage is assumed.

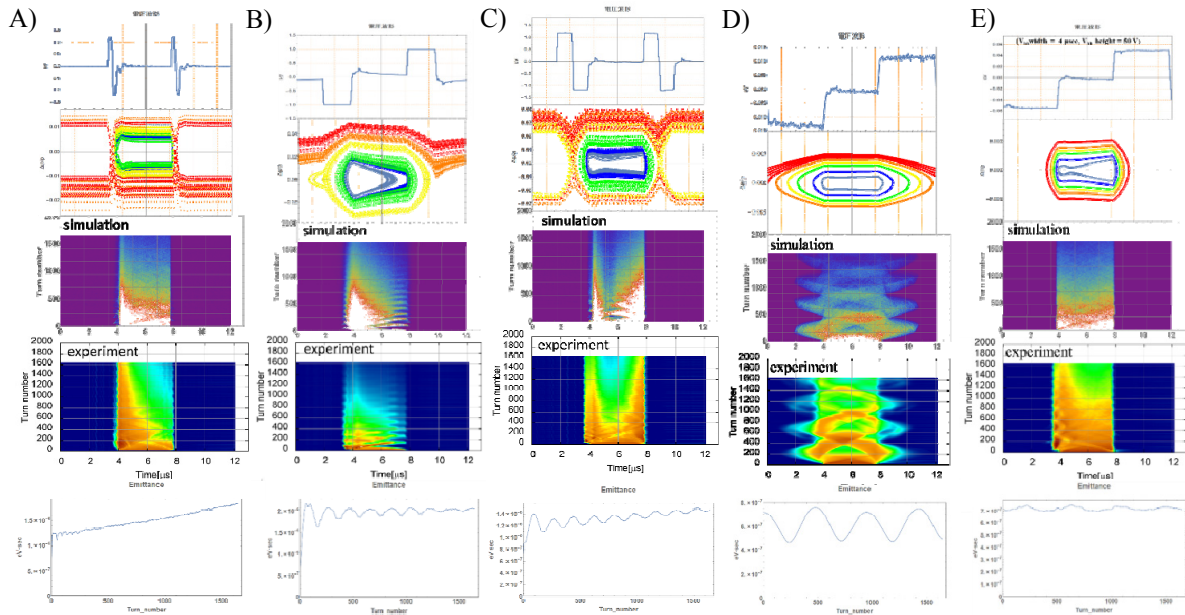


Figure5: Barrier voltage profile with reflections, phase space structure, bunch evolution in turn (simulation), bunch evolution in turn (experiment), and evolution of the emittance in turn. The parameters are shown in the Table 1.

In order to investigate the barrier voltage height dependence of emittance increasing in a more systematic way, the following simulation has been conducted. Assuming a typical waveform with t_f of 500 ns shown in Fig. 6 that has been actually realized in the experiment, the temporal evolution of the emittance has been calculated for the different heights. In the early stage of confinement, that is, the first few tenth turns, the emittances abruptly increase and then gradual increasing is observed for the voltage height exceeding 1 kV shown in the Fig. 7.

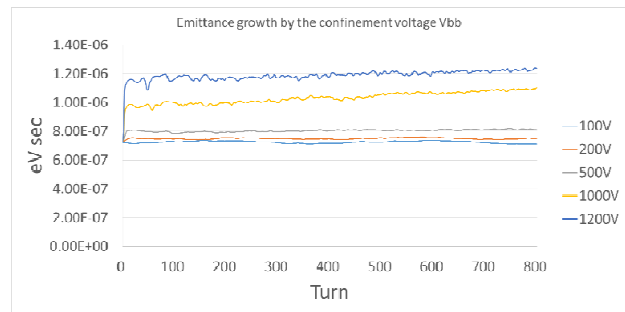


Figure7: Temporal evolution of emittance.

CONCLUSION

Dynamics for beam confinement has been manifested by means of the actual experiment in the KEK-DA and the numerical simulation. Its turns out that both results are fairly in good agreement with each other. The present studies suggest that it is quite important to optimize the barrier voltage profile including its height to avoid undesired emittance increasing.

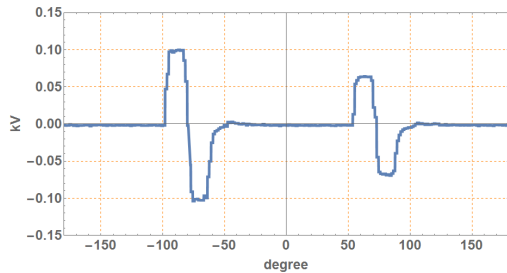


Figure6: Typical waveform of the barrier voltage.

REFERENCES

- [1] J. Griffin, C. Ankenbrandt, J. MacLachlan, and A. Moretti, "Isolated Bucket RF Systems in the Fermilab Antiproton Facility", IEEE Trans. Nucl. Sci. NS-30, 3502 (1983).
- [2] M. Blaskiewicz and J. Brennan, "A Barrier Bucket Experiment for Accumulating De-bunched Beam in the AGS", Proc. of EPAC1996, 2373 (1996).
- [3] C.M. Bhat, "Applications of Barrier Bucket RF Systems at FERMILAB", Proc. of Int. Workshop on Recent Progress in Induction Accelerators, Tsukuba, 45 (2006).
- [4] K. Takayama et al., "Experimental Demonstration of the Induction Synchrotron", Phys. Rev. Lett. 98, 054801 (2007).
- [5] K. Takayama, T. Yoshimoto, Liu Xingguang et al., "Induction Acceleration of Heavy Ions in the KEK Digital Accelerator: Demonstration of a Fast-Cycling Induction Synchrotron", Phys. Rev. ST-AB 17, 010101 1-6 (2014).